DFT Study of the Products, Potential Energy Surface, and Substituent Effects for Methyl Radical Addition to $[Rh(PMe_3)_2(CO)X]$ (X = Halogen or CN)

Nadeen H. Nsouli, Issaaf Mouawad, and Faraj Hasanayn*

Department of Chemistry, The American University of Beirut, Beirut, Lebanon

Received October 26, 2007

Methyl radical addition to [*trans*-$Rh(PMe_3)_2(CO)Cl$] (**1**) has been studied using density functional theory utilizing ECPs on the heavy elements. At the B3LYP level, ΔH_{298} for the transformation from separate reactants to the five-coordinate 17-e Rh−alkyl product (**2**) is −8.6 kcal/mol. On the other hand, ΔH_{298} for formation of the four-coordinate 15-e Rh−acyl radical (**3**) resulting from methyl addition to the carbonyl of **1** is −11.5 kcal/mol. The latter result implies that coordination of CO in **1** reduces the exothermicity of its reaction with CH_3 by 5.2 kcal/mol. A 3D potential energy surface of the given reaction reveals that the lowest energy path from separate reactants to **2** does not have any electronic barrier. Similarly, there is no distinct transition state for direct methyl attack on the carbonyl of **1**. Instead, the lowest energy trajectory connecting the separate reactants to the acyl product passes through a CO insertion transition state ($\mathbf{TS_{2,3}}$) corresponding to methyl migration between the rhodium and carbon atoms of the Rh−CO bond, with ΔH_{298} of $\mathbf{TS_{2,3}}$ being only 3.1 kcal/mol above the separate reactants. To explore the extent to which the methyl affinity of the coordinated carbonyl in the given system may change when the substituents on the metal are varied, additional calculations have been carried out on the F, Br, I, and CN analogues of **1**. Attempts have been made to account for the calculated methyl affinity trends using the ionization and Rh−CO bond dissociation energies of the square-planar reactants.

Introduction

The addition of alkyl radicals to unsaturated organic substrates provides an important methodology for carbon−carbon bond formation in organic and polymer chemistry.[1,2] The factors that determine the kinetics and thermodynamics of this reaction have been the subject of many experimental[3,4] and theoretical[5,6] investigations and were recently reviewed by Fischer and Radom.[7,8] Naturally, coordination of an unsaturated substrate to a metal will be expected to modify the chemistry of its reaction with free radicals. In fact, examples of syntheses utilizing alkyl radical addition to an arene,[9–11] allyl,[12,13] or carbene[14] coordinated to transition metals are known, and the topic has been reviewed.[15] However, there is still no general knowledge of how the nature of the metal or the coordination environment will affect the activation and reaction energies of addition of free radicals to metal-coordinated substrates.

Carbon monoxide is an example of an unsaturated substrate that reacts with alkyl radicals in the gas and solution phases (eq 1). The reversibility of the reaction is known to limit the use of carbon monoxide as a source to prepare free acyl radicals, and it also complicates the utility of independently generated acyl radicals in synthesis.[16,17]

* Corresponding author. E-mail: fh19@aub.edu.lb.

(1) (a) Giese, B. *Radicals in Organic Syntheses: Formation of Carbon-Carbon Bonds*; Pergamon: Oxford, England, 1986. (b) Curran, D. P. In *Comprehensive Organic Sythesis*; Trost, B. M., Flemming, I. M., Semmelhack, M. F., Eds.; Pergamon: Oxford, England, 1991; Vol. 4. (c) Fossey, J.; Lefort, D.; Sorba, J. *Free Radicals in Organic Chemistry*; Wiley: New York, 1995.

(2) (a) Kamigaito, M.; Ando, T.; Sawamoto, M. *Chem. Rev.* **2001**, *101*, 3689. (b) Matyjaszewski, K.; Xia, J. *Chem. Rev.* **2001**, *101*, 2921. (c) Hawker, C. J.; Bosma, A. W.; Harth, E. *Chem. Rev.* **2001**, *101*, 3661.

(3) (a) Zytowski, T.; Fischer, H. *J. Am. Chem. Soc.* **1996**, *118*, 437. (b) Fischer, H.; Zytowski, T. *J. Am. Chem. Soc.* **1997**, *119*, 12869. (c) Fischer, H.; Radom, L. *Angew. Chem., Int. Ed.* **2001**, *40*, 1340.

(4) (a) Beckwith, A. L.; J. Poole, J. S. *J. Am. Chem. Soc.* **2002**, *124*, 9489. (b) Kim, S. *Adv. Synth. Catal.* **2004**, *19*, 346. (c) Traeger, J. C.; Morton, T. H. *J. Phys. Chem. A* **2005**, *109*, 10467. (d) Lalevee, J.; Allonas, X.; Genet, S.; Fouassier, J.-P. *J. Am. Chem. Soc.* **2003**, *125*, 9377. (e) Lalevee, J.; Allonas, X.; Fouassier, J.-P. *J. Org. Chem.* **2005**, *70*, 814.

(5) (a) Henry, D. J.; Coote, M. L.; Gomez-Balderas, R.; Radom, L. *J. Am. Chem. Soc.* **2004**, *126*, 1732. (b) Gomez-Balderas, R.; Coote, M. L.; Henry, D. J.; Radom, L. *J. Phys. Chem. A* **2004**, *108*, 2874. (c) Wong, M. W.; Pross, A.; Radom, L. *J. Am. Chem. Soc.* **1994**, *116*, 6284. (d) Wong, M. W.; Pross, A.; Radom, L. *J. Am. Chem. Soc.* **1994**, *116*, 11938. (e) Wong, M. W.; Radom, L. *J. Phys. Chem.* **1995**, *99*, 8582.

(6) (a) Saeys, M.; Reyniers, M.-F.; Marin, G. B.; Van Speybroeck, V.; Waroquier, M. *J. Phys. Chem. A* **2003**, *107*, 9147. (b) Gonzalez, C.; Sosa, C.; Schlegel, H. B. *J. Phys. Chem.* **1989**, *93*, 2435. (c) Nguyen, H. M. T.; Peeters, J.; Nguyen, M. T. J.; Chandra Asit, K. *J. Phys. Chem. A* **2004**, *108*, 484. (d) Tokmakov, I. V.; Park, J.; Lin, M. C. *ChemPhysChem* **2005**, *6*, 2075. (e) Boyd, S. L.; Boyd, R. J. *J. Phys. Chem. A* **2001**, *105*, 7096.

(7) Fischer, H.; Radom, L. *Angew. Chem., Int. Ed.* **2001**, *40*, 1340.

(8) (a) Wong, M. W.; Radom, L. *J. Phys. Chem.* **1995**, *99*, 8582. (b) Wong, M. W.; Radom, L. *J. Phys. Chem. A* **1998**, *102*, 2237.

(9) (a) Schmalz, H-G.; Siegel, S.; Bats, J. W. *Angew. Chem., Int. Ed.* **1995**, *34*, 2383. (b) Merlic, C. A.; Walsh, J. C. *J. Org. Chem.* **2001**, *66*, 2276.

(10) (a) Lin, H.; Zhang, H.; Yang, L.; Li., C. *Org. Lett.* **2001**, *4*, 823. (b) Byers, J. H.; Jason, N. J. *Org. Lett.* **2006**, *8*, 3455.

(11) Merlic, C. A.; Miller, M. M.; Hietbrink, B. N.; Houk, K. N. *J. Am. Chem. Soc.* **2001**, *123*, 490.

(12) (a) Casty, G. L.; Stryker, J. M. *J. Am. Chem. Soc.* **1995**, *117*, 7814. (b) Ogoshi, S.; Stryker, J. M. *J. Am. Chem. Soc.* **1998**, *120*, 3514. (c) Carter, C. A. G.; McDonald, R.; Stryker, J. M. *Organometallics* **1999**, *18*, 820.

(13) (a) Simon, J.; Freeman, N. T.; Baird, M. C. *Chem. Commun.* **2000**, *18*, 1777. (b) Reid, S. J.; Baird, M. C. *J. Chem. Soc., Dalton Trans.* **2003**, *20*, 3975.

(14) Merlic, C. A.; Xu, D. *J. Am. Chem. Soc.* **1991**, *113*, 9855.

(15) Torraca, K. E.; McElwee-White, L. *Coord. Chem. Rev.* **2000**, *206–207*, 469.

(16) Chatgilialoglu, C.; Crich, D.; Komatsu, M.; Ryu, I. *Chem. Rev.* **1999**, *99*, 1991.

10.1021/om701079m CCC: $40.75
Publication on Web 04/02/2008

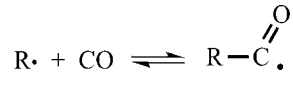

(1)

The reaction between an alkyl radical and CO would still be conceivable when CO is coordinated to a transition metal (eq 2). This reaction was invoked by Boese and Goldman to account for the observed activity of some alkane photocatalytic carbonylation systems mediated by d^8-metal–carbonyl complexes.[18]

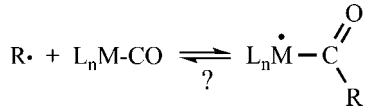

(2)

We have been interested in utilizing theoretical methods to investigate the transition state and products of alkyl radical addition to metal-coordinated ligands. To this end, we recently reported a study of alkyl addition to the series of [Mo(CO)$_6$], [Ru(CO)$_5$], [Ru(dmpe)(CO)$_3$], and [Pd(CO)$_4$] metal carbonyls.[19] In these systems, direct alkyl addition to the coordinated CO takes place via transition states that impart increased barriers to the reaction of the coordinated CO compared to free CO. Remarkably, the calculated activation and reaction energies followed different trends, with the thermodynamics being far more sensitive to the metal configuration than the kinetics. The previous study focused on electronically saturated complexes, but for the sake of comparison it included limited calculations on [Rh(CO)$_4$]$^+$ as a model for 16-e square-planar complexes.[19] Herein we extend the use of the electronic structure methods to study in more detail methyl addition to [*trans*-Rh(PMe$_3$)$_2$(CO)Cl] (**1**). Consideration of this prototype of square-planar complexes introduces important modifications to the reacting M−CO site that are likely to lead to a behavior different from that of any of the previously studied 18-e complexes. First, and as shown in Scheme 1, alkyl addition to the carbonyl of **1** affords a four-coordinate acyl product, **3**, that would be formally classified as a 15-e ML$_4$ metal radical. Because this is a rather uncommon class of compounds, it is not easy to speculate on how the energies of alkyl addition to the carbonyl of **1** will compare with those of addition to free CO or the previously studied metal carbonyls.

Furthermore, Scheme 1 shows that a free radical can in principle add to either the metal or the carbon of the M−CO bond. For the 18-e metal carbonyls, the metal−alkyl products were either much higher in energy than the 17-e metal−acyl products or unstable to CO dissociation.[19] Examination of Scheme 1 gives reason to anticipate a different scenario in the reaction of **1**, since in this case the Rh−alkyl product (**2**) will be the formally 17-e species. Finally, the possibility of substituting the chloride in **1** by other anionic ligands provides an opportunity to evaluate the extent by which small electronic perturbations within the same class of complexes may modify the reaction energy of alkyl addition to an M−CO bond.

Scheme 1. An Alkyl Radical Can Add to Either the Rh or CO of 1 (L = PMe$_3$)

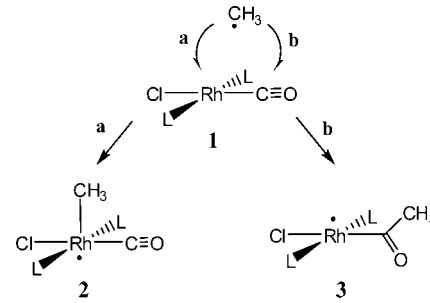

The new results (based on density functional theory)[20] predict that, even for **1**, alkyl addition to the carbonyl of **1** is thermodynamically more favored than addition to its Rh center, albeit by only a small extent. However, methyl addition to the carbonyl of **1** is 5 kcal/mol less exothermic than addition to free CO. In addressing the kinetics of the reaction we find that unlike the 18-e systems, there is no distinct transition state for direct methyl addition to the carbonyl of **1**. Finally, calculation of the F, Br, I, and CN analogues of **1** shows that the anionic ligand in this system exerts a small yet not insignificant effect on the methyl affinity of the coordinated carbonyl.

Computational Details

The calculations were performed at the B3LYP level[21] using Gaussian 03.[22] The doublet states were of the unrestricted type (UB3LYP). The Radom group had found this method to provide a cost-effective means to obtain satisfactory activation and reaction energies of free radical addition to organic unsaturated substrates.[7] To support some of the conclusions of the study, some calculations were repeated using the BPW91 functional.[23] In all calculations, the Gaussian 6-31G** standard basis set was used on H, C, N, O, and F.[24] The heavier elements carried the Hay−Wadt relativistic effective core potentials (ECPs) and the double-ζ basis set supplied with them (specified as LANL2DZ in Gaussian),[25] along with a set of 6d or 10f polarization functions with exponents 0.55 (P), 0.75 (Cl), (0.42) Br, 0.27 (I), and 0.4 (Rh). For phosphorus and the halogens, the given exponents were obtained from the Huzinaga

(17) (a) Jensen, C. M.; Lindsay, K. B.; Taaning, R. H.; Karaffa, J.; Hansen, A. M.; Skrydstrup, T. *J. Am. Chem. Soc.* **2005**, *127*, 6544. (b) Hansen, A. M.; Lindsay, K. B.; Antharjanam, S.; Karaffa, J.; Daasbjerg, K.; Flowers, R. A.; Skrydstrup, T. *J. Am. Chem. Soc.* **2006**, *128*, 9616. (c) Tojino, M.; Otsuka, N.; Fukuyama, T.; Matsubara, H.; Ryu, I. *J. Am. Chem. Soc.* **2006**, *128*, 7712.

(18) (a) Boese, W. T.; Goldman, A. S. *J. Am. Chem. Soc.* **1992**, *114*, 350. (b) Boese, W. T.; Goldman, A. S. *Tetrahedron Lett.* **1992**, *33*, 2119.

(19) Hasanayn, F.; Nsouli, N. H.; Al-Ayoubi, A.; Goldman, A. *J. Am. Chem. Soc.* **2008**, *130*, 511.

(20) Kohn, W.; Sham, L. J. *Phys. Rev. A* **1965**, *140*, 1133.

(21) (a) Becke, A. D. *Phys. Rev. B* **1988**, *37*, 785. (b) Lee, C.; Yang, W.; Parr, R. G. *Phys. Rev. B* **1988**, *37*, 785. (c) Johnson, B. G.; Gill, P. M. W.; Pople, J. A. *J. Chem. Phys.* **1993**, *98*, 5612. (d) Stephens, P. J.; Devlin, F. J.; Chabalowski, C. F.; Frisch, M. J. *J. Phys. Chem.* **1994**, *98*, 11623.

(22) Frisch, M. J.; Trucks, G. W.; Schlegel, H. B.; Scuseria, G. E.; Robb, M. A.; Cheeseman, J. R.; Montgomery, J. A., Jr. Vreven, T.; Kudin, K. N.; Burant, J. C. Millam, J. M.; Iyengar, S. S.; Tomasi, J.; Barone, V.; Mennucci, B.; Cossi, M.; Scalmani, G.; Rega, N.; Petersson, G. A.; Nakatsuji, H.; Hada, M.; Ehara, M.; Toyota, K.; Fukuda, R.; Hasegawa, J.; Ishida, M.; Nakajima, T.; Honda, Y.; Kitao, O.; Nakai, H.; Klene, M.; Li, X.; Knox, J. E.; Hratchian, H. P.; Cross, J. B.; Adamo, C.; Jaramillo, J.; Gomperts, R.; Stratmann, R. E.; Yazyev, O.; Austin, A. J.; Cammi, R.; Pomelli, C.; Ochterski, J. W.; Ayala, P. Y.; Morokuma, K.; Voth, G. A.; Salvador, P.; Dannenberg, J. J.; Zakrzewski, V. G.; Dapprich, S.; Daniels, A. D.; Strain, M. C.; Farkas, O.; Malick, D. K.; Rabuck, A. D.; Raghavachari, K.; Foresman, J. B.; Ortiz, J. V.; Cui, Q.; G. Baboul, A. G.; Clifford, S.; Cioslowski, J.; Stefanov, B. B.; Liu, G.; Liashenko, A.; Piskorz, P.; Komaromi, I.; Martin, R. L.; Fox, D. J.; Keith, T.; Al-Laham, M. A.; Peng, C. Y.; Nanayakkara, A.; Challacombe, M.; Gill, P. M. W.; Johnson, B.; Chen, W.; Wong, M. W.; Gonzalez, C.; Pople, J. A. *Gaussian 03, revision B.05*; Gaussian, Inc.: Pittsburgh, PA, 2003.

(23) Perdew, J. P.; Burke, K.; Wang, Y. *Phys. Rev. B* **1996**, *54*, 16533.

(24) (a) Rassolov, V. A.; Ratner, M. A.; Pople, J. A.; Redfern, P. C.; Curtiss, L. A. *J. Comput. Chem.* **2001**, *22*, 976. (b) Frisch, M. J.; Pople, J. A.; Binkley, J. S. *J. Chem. Phys.* **1984**, *80*, 3265.

(25) Hay, P. J.; Wadt, W. R. *J. Chem. Phys.* **1985**, *82*, 279.

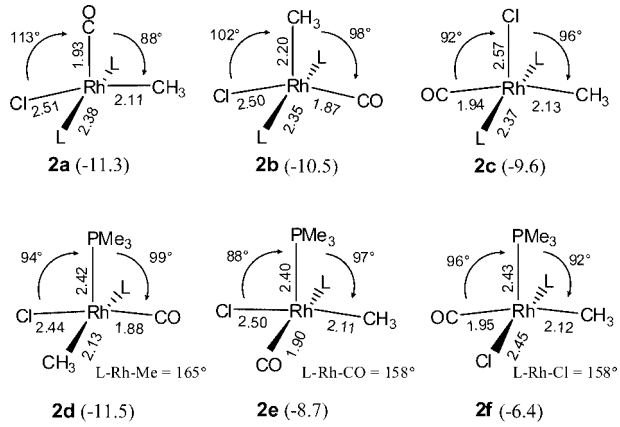

Figure 1. Geometrical parameters (in deg and Å) of the Rh−alkyl products from Me addition to **1** and their energy relative to the separate reactants (ΔE_{B3LYP} in kcal/mol; L = PMe_3).

basis set.[26] For Rh, the value of 0.4 was obtained by taking the 6-31G** f-polarization exponent of cobalt and dividing it by 2, on the basis that the exponents of the basis functions of the valence orbitals are generally smaller for the larger atoms. After completing this study, a referee drew our attention to a set of one-primitive polarization functions for the transition metals developed by the Frenking group by optimization of the atomic energies at the CISD level while using the LANL2DZ ECP.[27] In the Frenking basis set, the exponent for Rh is 1.35 (which is also half the f-exponent of Co in this basis set). For comparison, we repeated some calculations using Frenking's exponent. The absolute energies (E_{B3LYP}) for the individual reactant and both the alkyl and acyl product complexes obtained with $f = 1.35$ were systematically 3 kcal/mol *higher* than the absolute energies obtained from minimization with $f = 0.4$. However, the geometries and the reaction energies were essentially identical for the two exponents. Harmonic vibrational frequencies were used without scaling to obtain the enthalpy and entropy terms.[28] The spin densities (obtained by the Mulliken scheme)[29] used ROB3LYP wave functions. Finally, the molecular orbitals (MO) were displayed by GaussView using an isosurface of 0.05, and the potential energy surface (PES) was displayed using Matlab.

Results and Discussion

The Alkyl Product (2). In studying the five-coordinate Rh−alkyl product (**2**) resulting from CH_3 addition to the metal center of **1**, we identified two sets of complexes described schematically in Figure 1. Set 1 was minimized in the C_s point group, thus retaining the initial *trans*-$Rh(PMe_3)_2$ arrangement of **1**, and includes three minima, **2a**, **2b**, and **2c**, arranged in ascending energy order in Figure 1. The second set includes complexes in which the two phosphanes are *cis* (**2d**, **2e**, and **2f**).

To a first approximation, the minima identified for **2** may be classified as geometrical isomers of a square pyramid that are differentiated by the identity of the ligand at the apical position. However, some of the isomers exhibit a pronounced degree of deviation from the idealized square-pyramidal motif. For example, in the lowest energy *trans*-isomer, **2a**, the combination

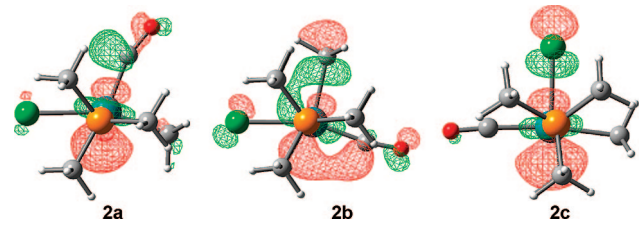

Figure 2. Display of the SOMO in **2a**, **2b**, and **2c**.

of 111° and 88° for the Cl−Rh−CO and CH_3−Rh−CO angles, respectively, is close to a trigonal-bipyramidal motif with the equatorial ligands in an asymmetrical distorted-Y arrangement. Such geometry is known for $[Rh(PR_3)_2(Cl)(H)(COPh)]$,[30] and other 16-electron closed-shell ML_5 organometallic complexes having a π-donor ligand.[31,32] Eisenstein and co-workers had shown that the symmetrical-Y and the distorted-Y geometries of d^6-ML_5 complexes can be related to distortion of the Jahn–Teller (JT) active closed-shell $^1E'$ state that is generated in the symmetrical D_{3h} geometry by the $(e'')^4(e')^2$ configuration of the d^6 electrons.[33] The same argument should be applicable to **2** since the $(e'')^4(e')^3$ electron configuration of a d^7-ML_5 complex in the D_{3h} point group affords the JT active $^2E'$ state. As demonstrated by Eisenstein[33] and others,[34,35] the geometrical details of JT-active organometallic compounds having hetero-ligands (as with the isomers of **2**) are strongly dependent on the electronic properties of the ligands involved in the distortion.

Despite the large electronic differences of the ligands, the three *trans*-isomers are calculated to have comparable energies. For example, **2b**, with the methyl group at the apical site, is less than a kcal/mol higher than **2a**, with apical CO. Similarly, the lowest energy *cis*-isomer (**2d**) has essentially the same energy as **2a**. Isomers **2e** and **2f** on the other hand are 1.8 and 3.2 kcal/mol higher in energy than **2a** (E_{B3LYP} energies without ZPE correction). When the entropy and enthalpy terms are included, **2d** becomes 1.5 kcal/mol higher in energy than **2a** (ΔG_{298}). For convenience, subsequent discussion will consider only the *trans*-isomers.

In all of the minima of **2**, the unpaired electron is calculated to be in a metal-based orbital having antibonding character due to σ-interaction with the "apical" ligand. This is illustrated in the display of the singly occupied MOs (SOMOs) of **2a**, **2b**, and **2c** in Figure 2. For **2b** the SOMO also has a significant in-phase mixing with the π^*-MO of the carbonyl, and consistently, Mulliken analysis allocates 16% of the spin density to

(26) Huzinaga, S., Ed. *Gaussian Basis Sets for Molecular Calculations*; Elsevier:, Amsterdam, The Netherlands, 1984..
(27) Ehlers, A. W.; B̈; ohme, M.; Dapprich, S.; Gobbi, A.; Höllwarth, A.; Jonas, V.; Köhler, K. F.; Stegmann, R.; Veldkamp, A.; Frenking, G. *Chem. Phys. Lett.* **1993**, *208*, 111.
(28) Hehre, W. J.; Radom, L.; Schleyer, P. v. R. PopleJ. A. *Ab Initio Molecular Orbital Theory*; Wiley: New York, 1986.
(29) Mulliken, R. S. *J. Chem. Phys.* **1934**, *2*, 782.
(30) Wang, K.; Emge, T. J.; Goldman, A. S.; Li, C.; Nolan, S. P. *Organometallics* **1995**, *14*, 4929.
(31) (a) Luder, D. M.; Lobkovsky, E. B.; Streib, W. E.; Caulton, K. G. *J. Am. Chem. Soc.* **1991**, *113*, 1837. (b) Lam, W. H.; Shimada, S.; Batsanov, A. S.; Lin, Z.; Marder, T. B.; Cowan, J. A.; Howard, K.; Sax, A.; Mason, G.; McIntyre, J. *Organometallics* **2003**, *22*, 4557.
(32) (a) Fryzuk, M. D.; MacNeil, P. A. *Organometallics* **1983**, *2*, 682. (b) Fryzuk, M. D.; MacNeil, P. A.; Ball, R. G. *J.Am. Chem. Soc.* **19861**, *08*, 6414. (c) Werner, H.; Hohn, A.; Dziallas, M. *Angew. Chem., Int. Ed.* **1986**, *25*, 1090. (d) Westcott, S. A.; Taylor, N. J.; Marder, T. B.; Baker, R. T.; Jones, N. J.; Calabrese, J. C. *J. Chem. Soc., Chem. Commun.* **1991**, 304. (e) Abdur-Rashid, K.; Clapham, S. E.; Hadzovic, A.; Harvey, J. N.; Lough, A. J.; Morris, R. H. *J. Am. Chem. Soc.* **2002**, *124*, 15104.
(33) (a) El-Idrissi, I.; Eisenstein, O.; Jean, Y. *New J. Chem.* **1990**, *14*, 671. (b) Riehl, J.; Jean, Y.; Eisenstein, O.; Pelissier, M. *Organometallics* **1992**, *11*, 729.
(34) (a) Abu-Hasanayn, F.; Cheong, P.; Oliff, M. *Angew. Chem., Int. Ed.* **2002**, *41*, 2120. (b) Hasanayn, F.; Markarian, M.; Al-Rifai, R. *Inorg. Chem.* **2004**, *43*, 3691.
(35) (a) Jensen, V. R.; Poli, R. *J. Phys. Chem. A* **2003**, *107*, 1424. (b) Poli, R. *Chem. Rev.* **1996**, *96*, 2135. (c) Harvey, J. N.; Poli, R.; Smith, K. *Coord. Chem. Rev.* **2003**, 238. (d) Poli, R.; Cacelli, I. *Eur. J. Inorg. Chem.* **2005**, *12*, 2324.

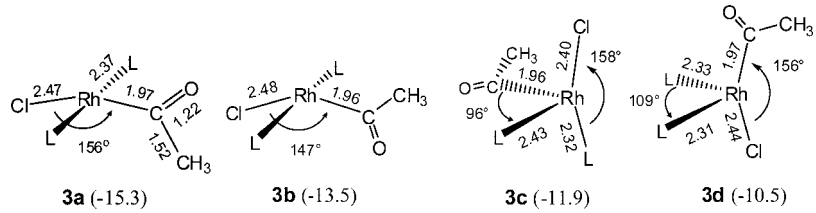

Figure 3. Geometrical parameters (in deg and Å) of the Rh−acyl products from CH_3 addition to **1** and their energy relative to the separate reactants (ΔE_{B3LYP} in kcal/mol; L = PMe_3).

the CO group of **2b**. In **2a** and **2c** on the other hand, the spin density is nearly totally allocated to the metal and the apical ligand. The isomers of **2** can therefore be classified as 17-e metal-based radicals, which are distinguished from the ligand-based radicals that are known for some organometallic radicals.[36,37]

Doublet State of the Acyl Product (3). The product resulting from CH_3 addition to the carbonyl of **1** (**3**, Scheme 1) would be formally classified as a d^7 15-e Rh(II) tetracoordinate metal radical. Except for the Co(II) halide complexes, $[CoX_4]^{2-}$, which are known to have quartet spin ground state and tetrahedral geometry,[38] we are not aware of fully characterized d^7-ML_4 complexes. Prior theoretical studies of d^7-ML_4 organometallic compounds were limited mostly to the $[M(CO)_4]$ system. Burdett[39] and Pensak[40] for example studied the doublet state of $[Mn(CO)_4]$ by the extended Hückel theory. More recent DFT calculations by Bauschlicher predicted the doublet and quartet spin states of $[Fe(CO)_4^+]$[41] and $[Mn(CO)_4]$[42] to have close energies, although the reported doublet state of $[Fe(CO)_4^+]$ was $^2A_{1g}$ with a square-planar geometry, while that of $[Mn(CO)_4]$ was $^2B_2$ with a distorted tetrahedral C_{2v} geometry. Thus in calculating our Rh−acyl product (**3**), we considered both the doublet and quartet states.

In searching for minima on the doublet energy surface of our acyl species (**3**), geometry minimization was started at square-planar, distorted tetrahedral and trigonal pyramidal initial geometries. This approach afforded four minima described in Figure 3, where they are arranged in an ascending energy order. The lowest energy Rh−acyl species in Figure 3 (**3a**) has a distorted square-planar geometry with the Cl−Rh−acyl angle of 156°. **3b** is related to **3a** by rotation of the acyl group by 180° along the Rh−C bond and exhibits a more pronounced bending of the Cl−Rh−acyl angle (147°). We note that the energy needed to linearize the Cl−Rh−acyl angle is only 1 kcal/mol above **3b**. This makes it hard to speculate on the cause of bending in this molecule.

In contrast to **3a** and **3b**, **3c** and **3d** have distorted tetrahedral geometries obtained by opening one angle of the idealized tetrahedral frame and closing another. In **3c**, Cl and a phosphane take the sites of the larger angle (158°), whereas in **3d** the larger angle (158°) is made by Cl and the acyl ligand. As is illustrated in the SOMO of **3a** and **3d** in Figure 4 (both calculated in the C_s point group), the two geometries of **3** correspond to two electronic states differentiated by the orbital configuration of the d^7 electrons. A complete qualitative MO energy level diagram

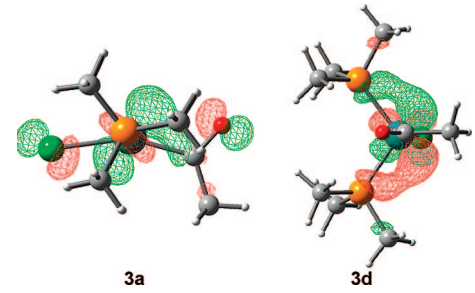

Figure 4. Comparison of the SOMO in **3a** and **3d**.

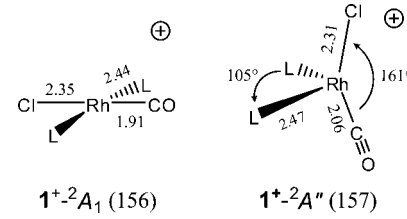

Figure 5. Geometrical parameters (in deg and Å, L = PMe_3) of the low-energy electronic states of the cation of **1** and ΔE_{B3LYP} (in kcal/mol) of their formation by ionization of **1**.

that correlates the d orbital in the two geometries can be found in a study by Elian and Hoffmann of transition metal fragments.[43]

In **3a** the d^7 configuration is $(a')^2(a'')^2(a'')^2(a')^1$ with the unpaired electron in an MO having largely d_{z2} character, thus affording an $^2A'$ state that matches the $^2A_{1g}$ state reported for $[Fe(CO)_4]^+$ in D_{4h}. In **3d** on the other hand the d^7 configuration is $(a')^2(a'')^2(a')^2(a'')^1$, which affords an $^2A''$ state related to the $^2B_2$ state reported for $[Mn(CO)_4]$. In **3d** the SOMO has d_{xz} character with pronounced mixing with the out-of-phase ligand group orbital of the two equivalent phosphanes (Figure 4).

Although **3a** and **3c** have different electronic states, their energies differ by only 3.3 kcal/mol. This highlights the importance of considering explicitly more than one electronic state (same multiplicity) in theoretical studies of unsaturated organometallic fragments. In such fragments, it is not unlikely for the energy order of the different states to reverse when the substituents are changed.[34b] As a matter of fact, the results obtained for **3a** and **3c** have led us to calculate two states of the cation radical of **1** (**1**$^+$), an $^2A_1$ state with a square-planar C_{2v} geometry and an $^2A''$ state with a tetrahedrally distorted C_s structure (Figure 5). In the past only the square-planar geometry was considered for this cation.[44] The new calculations predict the two states to have nearly the same energy.

Quartet State of the Acyl Product (3e and 3f). As mentioned before, d^7-ML_4 complexes have an accessible quartet

(36) Astruc, D. *Acc. Chem. Res.* **1991**, *24*, 36.
(37) de Bruin, B.; Russcher, J. C.; Gruetzmacher, H. *J. Organomet. Chem.* **2007**, *692*, 3167.
(38) Cotton, F. A.; Wilkinson, G. *Advanced Inorganic Chemistry*, 5th ed.; Wiley: New York, 1988; p 729.
(39) Burdett, J. K. *J. Chem. Soc., Faraday Trans. 2* **1974**, *70*, 1599.
(40) Pensak, D. A.; McKinney, R. J. *Inorg. Chem.* **1979**, *18*, 3407.
(41) Andrews, L.; Zhou, M.; Wang, X.; Bauschlicher, C. W., Jr. *J. Phys. Chem. A* **2000**, *104*, 8887.
(42) Ricca, A.; Bauschlicher, C. W., Jr. *J. Phys. Chem.* **1994**, *98*, 12899.
(43) Elian, M.; Hoffmann, R. *Inorg. Chem.* **1975**, *14*, 1058.
(44) (a) Abu-Hasanayn, F.; Krogh-Jespersen, K.; Goldman, A. *Inorg. Chem.* **1993**, *32*, 495. (b) Abu-Hasanayn, F.; Goldman, A.; Krogh-Jespersen, K. *Inorg. Chem.* **1994**, *33*, 5122.

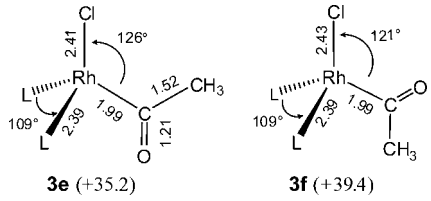

Figure 6. Selected parameters (deg and Å, L = PMe_3) of the quartet state of the product from CH_3 addition to the carbonyl of **1** and their energy relative to the doublet state (**3a**).

Table 1. Reaction Energy of CH_3 Addition to Metal-Coordinated Carbonyls and Possible Correlation with the Ionization (IE) and Carbonyl Bond Dissociation (BDE) Energies[a]

rxn of	E_{B3LYP}	$\Delta H_{298}°$	IE[b]	BDE[c]
→**1** (→ **2a**)	−11.3	−8.6		
1 (→ **3a**)	15.3	−11.5	156	63.5 (**T1**) 49.0 (**T2**)
free CO	−19.9	−16.2		
$[Mo(CO)_6]$	−7.9	−4.3	192	38.2 (C_{4v})
$[Ru(CO)_5]$	−25.6	−21.4	172	26.4 (C_{2v})
$[Pd(CO)_4]$	−21.8	−17.8	186	9.3 (D_{3h})
$Ru(dmpe)(CO)_3]$	−27.1	−22.8	139	34.2 (C_1)

[a] Units are in kcal/mol. ΔE_{B3LYP} is the raw electronic energy for the transformation from separate reactants to the products and is given without ZPE correction. $\Delta H_{298}°$ is the standard state enthalpy of the reaction at 298 K and 1 atm. Data for the 18-e complexes are reproduced from ref 19. [b] IE is the ionization energy of the reactant (ΔE_{B3LYP}). The point group of the ionized products is square-planar C_{2v} (**1**), D_{2d} (Mo), C_{4v} (Ru), and C_{3v} (Pd). [c] BDE is the CO bond dissociation energy (ΔE_{B3LYP}) of the reactant metal carbonyl leading to the fragment with the specified point group. **T1** and **T2** are the *trans*- and *cis*-isomers, respectively, of the $[Rh(PMe_3)_2(Cl)]$ fragment.

spin state. In studying this state for the acyl complex from methyl addition to **1** two minima were identified, **3e** and **3f** in Figure 6.

Not unexpectedly, the geometry of this open-shell state is near tetrahedral. However, at the B3LYP level, **3e** is 35 kcal/mol higher in energy than **3a**. This is in contrast with the $[Fe(CO)_4]^+$ and $[Mn(CO)_4]$ systems, where previous DFT calculations predicted small doublet-quartet gaps. Both the identity of the metal and the nature of the ligands are likely to play a role in increasing the doublet-quartet gap in **3**. In particular, the first-row transition metals are known to favor open-shell configurations more than the second-row metals.[45] The 35 kcal/mol gap between the two spin states in **3** implies that the quartet state is unlikely to play any significant role in the thermal chemistry of **3**, and thus will not be discussed in the remaining part of the study.

Reaction Thermodynamics and Comparison with Other Systems. An objective of our study has been to identity the likely thermodynamic product from CH_3 addition to **1** and to compare the energy of formation of the acyl product with the energy of methyl addition to free CO and to the previously studied 18-e metal carbonyls. The analysis will be based on the lowest energy isomer of each of the alkyl (*trans*-isomer) and acyl species, **2a** and **3a**, respectively. The relevant data are presented in Table 1. The Table shows that ΔH_{B3LYP} for formation of **2a** and **3a** from the separate reactants is −8.6 and −11.5 kcal/mol, respectively (at 298 K). Adding the entropy terms for the given bimolecular associative transformations gives ΔG_{B3LYP} = +0.8 and −2.6 kcal/mol for formation of **2a** and **3a**, respectively (at 298 K). When the BPW91 functional is used in the calculations, the respective reaction enthalpies become −11.1 (**2a**) and −12.6 (**3a**) kcal/mol. These DFT-based results mean that the unconventional 15-e four-coordinate metal−acyl radical is lower in energy than the metal−alkyl product, which belongs to the more common class of 17-e pentacoordinate organometallic radicals.[46,47] However, considering the very different nature of the Rh−C and C−C bonds being made, the calculated energy difference between **2a** and **3a** may be too small to allow making a strong predictive statement on the thermodynamic product of the given reaction.[48]

Compared to the calculated energy of methyl addition to free CO (ΔH_{B3LYP} = −16.2 kcal/mol), the calculations indicate that CO coordination in **1** reduces the driving force of its reaction with the methyl radical by 4.7 kcal/mol. This is the opposite of the effect of coordination in $[Ru(CO)_5]$ or $[Pd(CO)_4]$, where the exothermicity is increased by 5.2 or 1.6 kcal/mol, respectively. However, methyl addition to **1** is still substantially more favored than addition to $[Mo(CO)_6]$ (ΔH_{B3LYP} = −4.3 kcal/mol, Table 1).

In our attempt to identify fundamental properties that are likely to play a role in determining the relative energy of alkyl radical addition to a coordinated CO, we previously searched for possible correlation between the calculated exothermicities of methyl addition and either the ionization or the M−CO bond dissociation energies of the metal carbonyl (IE and BDE, respectively; Table 1). The IE was thought to be relevant because alkyl addition to a metal-coordinated carbonyl is (at least formally) oxidative in the metal, and the reaction can be broken into an electron transfer cycle incorporating ionization of the metal complex as shown in eq 3.

$$[M(CO)_n] + [CH_3] \rightarrow [M(CO)_n]^+ + [CH_3]^- \rightarrow [M(CO)_{n-1}COCH_3] \quad (3)$$

For the three penultimate metal carbonyls we found a qualitative correlation between the trends in the exothermicities of methyl addition and the ionization energy of the metal carbonyl: $-\Delta E_{B3LYP}$ = 7.9 (Mo) < 25.6 (Ru) > 21.8 (Pd), vs IE = 192 (Mo) > 172 (Ru) < 189 (Pd) (in kcal/mol), with the easier to ionize complexes showing the greater methyl affinity (data reproduced in Table 1). However, for $[Ru(dmpe)(CO)_3]$ the calculated IE was some 30 kcal/mol smaller than the IE of $[Ru(CO)_5]$, yet it added the methyl radical only slightly more favorably ($\Delta\Delta E$ = 1.5 kcal/mol). The idea behind examining the M−CO bond strength was then that alkyl addition to an M−CO bond can be expressed as the sum of M−CO bond dissociation and M−acyl bond formation as shown in eq 4. According to this equation, a stronger M−CO bond should disfavor methyl addition.

(45) Huheey, J. E.; Keiter, E. A.; Keiter, R. L. *Inorganic Chemistry, Principles of Structure and Reactivity*, 4th ed.; Harper Collins: New York, 1993.

(46) Fortier, S.; Baird, M. C.; Preston, K. F.; Morton, J. R.; Ziegler, T.; Jaeger, T. J.; Watkins, W. C.; MacNeil, J. H.; Watson, K. A. *J. Am. Chem. Soc.* **1991**, *113*, 542. (b) O'Callaghan, K. A. E.; Brown, S. J.; Page, J. A.; Baird, M. C.; Richards, T. C.; Geiger, W. E. *Organometallics* **1991**, *10*, 3119. (c) MacConnachie, C. A.; Nelson, J. M.; Baird, M. C. *Organometallics* **1992**, *11*, 2521. (d) Kuksis, I.; Baird, M. C. *Organometallics* **1994**, *13*, 1551. (e) Koeslag, M. A.; Baird, M. C.; Lovelace, S.; Geiger, W. E. *Organometallics* **1996**, *15*, 3289. (f) Kuksis, I.; Kovacs, I.; Baird, M. C.; Preston, K. F. *Organometallics* **1996**, *15*, 4991.

(47) (a) Fryzuk, M. D.; Leznoff, D. B.; Rettig, S. J. *Organometallics* **1997**, *16*, 5116. (b) Alonso, P. J.; Fornies, J.; Garcia-Monforte, M. A.; Martin, A.; Menjon, B. *Organometallics* **2005**, *24*, 1269.

(48) We note that at the B3LYP level methyl addition to the carbonyl of $[RhCO)_4]^+$ is 10 kcal/mol more preferred over addition to the Rh center. However, this preference is reduced to a kcal/mol at the CCSD-T level (ref 19). Unfortunately there is currently no experimental data to evaluate which method is the more accurate for the given problem. The size of the two radical products from $[RhPMe_3)_2CO)Cl]$ precluded application of the CCSD-T level.

$$[M(CO)_n] \rightarrow [M(CO)_{n-1}] + CO \quad (4a)$$

$$[M(CO)_{n-1}] + \cdot C(O)CH_3 \rightarrow [M(CO)_{n-1}(COCH_3)] \quad (4b)$$

The M−CO bond dissociation energy trends (BDE, Table 1) of the three penultimate metal carbonyls did not correlate with their CO methyl affinities. Nonetheless, for [Ru(dmpe)(CO)$_3$] the BDE was 8 kcal greater than the BDE of [Ru(CO)$_5$]. The increased Ru−CO BDE in [Ru(dmpe)(CO)$_3$] can therefore be thought of as a factor that counteracts the presumably favorable effect of its low IE on CH_3 addition.

The new result for methyl addition to the carbonyl of **1** provides an additional system to evaluate more critically the relevance of the IE and BDE on the thermodynamics of methyl addition to an M−CO bond. The calculated IE of **1** is 156 kcal/mol, substantially smaller than the IE of [Ru(CO)$_5$] (172 kcal/mol). Again, based on this parameter alone and the premise that methyl addition to the carbon of the M−CO bond is oxidative in the metal, one would have expected the carbonyl of **1** to have a much greater methyl affinity than [Ru(CO)$_5$], contrary to the calculated results. Thus the new calculations on **1** give an unambiguous example that shows that the ionization energy is not the only decisive factor in determining the relative methyl affinity of metal-coordinated CO. As argued for [Ru(dmpe)(CO)$_3$], this failure of the IE to account for the relative methyl affinity of [Rh(PMe$_3$)$_2$(CO)Cl] and [Ru(CO)$_5$] can be accounted for based on the relative strength of the M−CO bond of the two complexes. Experimentally, **1** is known to have an exceptionally strong M−CO bond.[49] The [Rh(PMe$_3$)$_2$Cl] fragment produced in CO dissociation from **1** has a T geometry that defines two isomers depending on whether the phosphanes are *trans* or *cis*.[50] Although the *cis*-isomer is the lower energy one,[50] the BDE of **1** leading to the *trans*-isomer should be more relevant to the analysis of methyl addition to **1**. Our calculated CO BDE from **1** to the *trans*-isomer (**T1** in Table 1) is 63.5 kcal/mol. This is 37 kcal/mol greater than the calculated BDE of [Ru(CO)$_5$], which can be easily large to reverse the greater methyl affinity of **1** that would have been anticipated on the basis of the relative IEs alone. The idea that interplay between the IE and BDE of M−CO bonds can satisfactorily account for the trends of their methyl affinities is supported further in the section on the substituent effects presented later in the study.

Potential Energy Surface of Methyl Addition to 1. Despite the greater thermodynamic driving force of methyl addition to a carbonyl coordinated in [Ru(CO)$_5$] compared to addition to free CO, the reaction of [Ru(CO)$_5$] was calculated to encounter an increased activation barrier of 5 kcal/mol. Given the reduced exothermicity of methyl addition to the carbonyl of **1**, it became of interest to know if the reaction will also have an increased kinetic barrier or not. To address this issue, we first attempted to locate a transition state (TS) for direct C−C bond formation between the methyl radical and the CO coordinated in **1** by conducting several TS minimizations starting at varied initial geometries based on the structure of the TSs previously identified for methyl addition to free CO and to the 18-e metal carbonyls. However, none of these searches converged satisfactorily to a first-order stationary point. We therefore reverted to calculating a detailed 3D potential energy surface, PES, defined as a function of the CH_3−Rh (r_{CM}) and CH_3−CO (r_{CC}) coordinates. In calculating this surface, the methyl group was brought to **1** in the Cl−Rh−CO plane but without imposing the C_s symmetry constraint. Our approach in constructing the surface was to consider one slice defined by a fixed r_{CM} value at a time. For each slice, the geometry was first minimized at the longest CC distance (3.4 Å), and the resulting parameters were then used for the next minimization at a shorter r_{CC} and so on. The analysis considered 247 points. The results are presented using surface and contour plots in Figure 7.

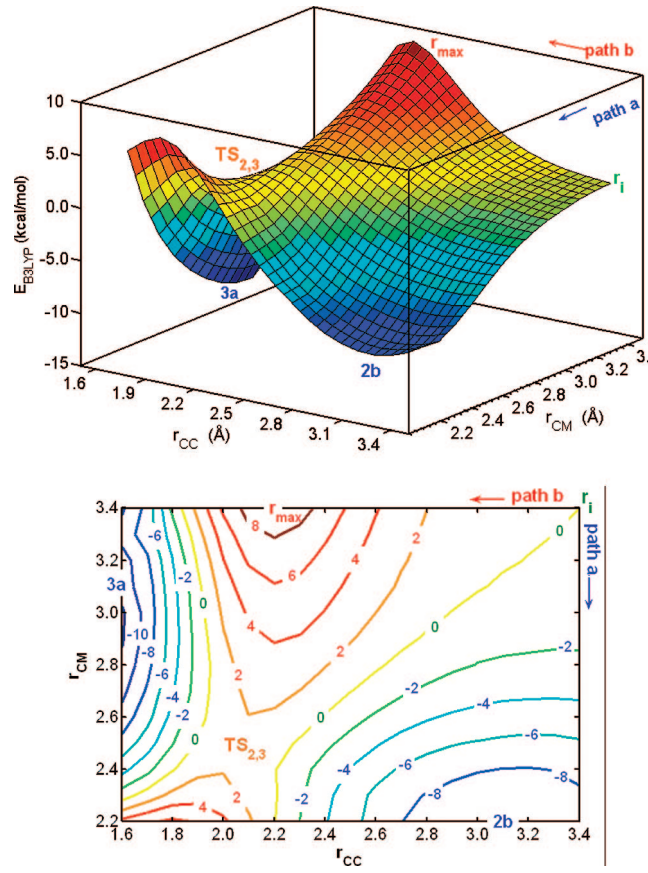

Figure 7. B3LYP potential energy surface for CH_3 addition to **1** and its contour projection.

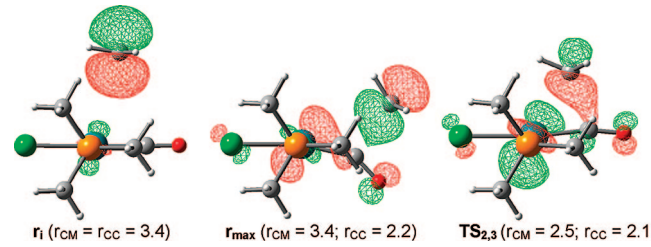

Figure 8. SOMO at $\mathbf{r_i}$, $\mathbf{r_{max}}$, and $\mathbf{TS_{2,3}}$ on the PES given in Figure 7 (parameters are in Å).

The point representing the initial stage of the reaction on the PES is $\mathbf{r_i}$, with r_{CM} and r_{CC} each at 3.4 Å. At this point there is essentially no change in the initial geometrical parameters characterizing the separate reactants (**1** and CH_3). Nonetheless, the SOMO at $\mathbf{r_i}$ reveals that the p_z-AO of the methyl group has already started to mix with the d_{z^2} AO of Rh (Figure 8). Consistently, at $\mathbf{r_i}$, Mulliken analysis allocates 6% of the spin density to the Rh atom.

(49) Rosini, G. P.; Liu, F.; Krogh-Jespersen, K.; Goldman, A. S.; Li, C.; Nolan, S. P. *J. Am. Chem. Soc.* **1998**, *120*, 9256.

(50) (a) Koga, N.; Morokuma, K. *J. Phys. Chem.* **1990**, *94*, 5454. (b) Margl, P.; Ziegler, T.; Bloechl, P. E. *J. Am. Chem. Soc.* **1995**, *117*, 12625. (c) Czerw, M.; Whittingham, T. K.; Krogh-Jespersen, K. In *Computational Organometallic Chemistry*; Cundari, T. R., Ed.; Marcel Dekker Inc.: New York, 2001.

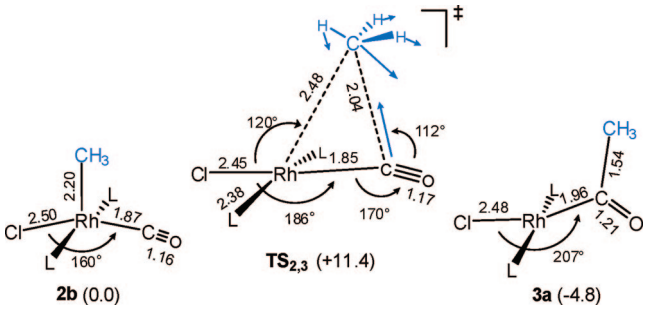

Figure 9. Geometric parameters (in Å) and vector components of the imaginary frequency of $\mathbf{TS_{2,3}}$. Energy values (E_{B3LYP}; in kcal/mol) are given relative to **2b**.

From $\mathbf{r_i}$, direct addition of CH_3 to the Rh center of **1** would be represented by the trajectory that retains long C−C distances (path a in Figure 7). This path leads to **2b**, the Rh−alkyl product with apical CH_3 (Figure 1). Clearly, there is no electronic barrier along this trajectory. This is perhaps not surprising since the alignment of the frontier orbitals involved in making the CH_3−Rh bond (the filled $4d_{z^2}$ and the empty $5d_z$) is provided along this path without the need for prior structural or electronic rearrangements from either reactant.

In contrast to path a, methyl addition to the carbonyl of **1** along the trajectory defined by the longest C−Rh distance (r_{CM} = 3.4 Å; path b in Figure 7) goes significantly uphill (by 8.7 kcal/mol) before it descends to the Rh−acyl radical (**3a**). At the highest point on this path ($\mathbf{r_{max}}$) r_{CC} is 2.2 Å. At this C−C distance the SOMO starts to include a minor component from the carbonyl π^* MO, but overall it is still dominated by the methyl-p_z and the metal-d_{z^2} AOs that characterize the SOMO at $\mathbf{r_i}$ (Figure 8). Interestingly, the values of r_{CM} and r_{CC} at $\mathbf{r_{max}}$, as well as the degree to which the Rh−C−O bond is bent (147°), are in close proximity to the values of the respective parameters in the TSs of methyl addition to CO coordinated in 18-e complexes. However, $\mathbf{r_{max}}$ is not a true TS, but is more like a second-order saddle point, where in addition to the coordinate of C−C bond formation, the energy goes down by shortening the CH_3−Rh bond. This provides an alternative lowest energy path to C−C bond formation that avoids $\mathbf{r_{max}}$ altogether and passes instead through a saddle point ($\mathbf{TS_{2,3}}$) at r_{CM} and r_{CC} bond distances of 2.48 and 2.04 Å, respectively (values are from full TS-geometry minimization). $\mathbf{TS_{2,3}}$ is a true TS characterized by one imaginary frequency ($\nu^{\ddagger}$= 323i cm^{-1}) having coordinates for methyl translation between the metal and the carbonyl as described in Figure 9.

All of the angular parameters in $\mathbf{TS_{2,3}}$ are intermediate between their respective values in **2b** and **3a**. For example, the Cl−Rh−CO angle varies from 160° in **2b** to 186° in $\mathbf{TS_{2,3}}$ and finally to 207° in **3a**. A particularly important structural feature in $\mathbf{TS_{2,3}}$ is the large degree of pyramidalization in the methyl moiety, which is the characteristic equilibrium geometry of the methyl anion. The nonradical character of the methyl group in $\mathbf{TS_{2,3}}$ is also supported by the SOMO, which has its largest component from the metal d_{z^2} AO (Figure 8), and by Mulliken analysis, which allocates a spin density of 0.54 to the metal center at this point. Thus, although there is evidently a large degree of spin delocalization in $\mathbf{TS_{2,3}}$, the calculated geometry and electronic structure of $\mathbf{TS_{2,3}}$ are most consistent with a conventional carbonyl insertion TS in which the methyl group has anionic character.

At the B3LYP level, the electronic energy of $\mathbf{TS_{2,3}}$ is only 0.5 kcal/mol above the reactants. Adding the ZPE and thermal terms at 298 K affords an enthalpy difference of 3.1 kcal/mol between $\mathbf{TS_{2,3}}$ and the reactants. Finally, and as would be expected from an associative reaction, the entropy terms ($-T\Delta S$) calculated at 298 K add approximately 10 kcal/mol to the energy of $\mathbf{TS_{2,3}}$ relative to the separate reactants, yielding $\Delta G^{\ddagger}_{298}$ = 13.8 kcal/mol. Since comparable enthalpy and entropy components are expected along paths a and b, the small electronic energy of $\mathbf{TS_{2,3}}$ relative to the reactants means that reaching $\mathbf{TS_{2,3}}$ on the PES may compete with direct formation of the Rh−alkyl product. Under such conditions, the kinetic distribution of the acyl and alkyl products will probably be determined by dynamic details including vibrational and entropy effects, as well as the steepness of the surface in the direction of **2b** and **3a**.[51] Although accounting for dynamic effects is beyond the scope of the present study, in the limiting conditions in which **2b** is produced as the only kinetic product, formation of the acyl product (**3a**) will depend on the activation energy of the insertion reaction connecting **2b** to **3a** via $\mathbf{TS_{2,3}}$. The calculated $\Delta E^{\ddagger}$ and $\Delta G^{\ddagger}_{298}$ values for this step are 11.4 and 11.9 kcal/mol, respectively, implying the reaction should be quite facile. Note, the geometry of $\mathbf{TS_{2,3}}$ is consistent with an early TS in the direction from **2** to **3**, with the Rh−CH_3 bond (2.48 Å) being only slightly longer than its value in the reactant **2b** (2.20 Å, Figure 9).

In brief, the calculations presented in this section do not support the existence of a distinct TS on the PES of methyl addition to the carbonyl of **1**. This contrasts with methyl addition to the ML_4, ML_5, and ML_6 18-e metal carbonyls, where the reactions are systematically characterized by TSs that impart increased activation energies for C−C bond formation compared to the reaction of free CO, even when the thermodynamics is highly favored. The different behavior of **1** can be attributed to its unique geometry and electronic structure compared to the other complexes. The square-planar geometry of **1** makes the valence AOs of Rh (the filled d_{z^2} and empty p_z) accessible for a net bonding interaction with the methyl radical at an early stage of the reaction (three-electron−three-orbital problem) without any requirement for distortion. This provides a barrierless energy path from the region on the PES where one would normally expect to find a transition state for C−C bond formation in the direction of Rh−C bond formation. In the 18-e complexes on the other hand, the ligands are spherically distributed, and the filled d orbitals are degenerate and oriented between the ligands. Furthermore, there are no empty p-AOs on the metal. Simplistically, therefore, the early stage of addition of a free radical to a metal center of an 18-e complex may be viewed as an antibonding three-electron two-orbital problem. In support of this view, we find that in sharp contrast to the reaction of **1**, when CH_3 is brought in the equatorial plane of $[Ru(CO)_5]$ to make a Ru−CH_3 bond, the energy initially goes uphill and drops down only when an ancillary CO is dissociated from the complex.[52] Such features in the 18-e systems seem to prevent skewing the PES around the C−C bond making TS in the direction of the metal.

Substituent Effects. Table 1 above compares the reaction energy of methyl radical addition to metal-coordinated CO in which both the geometry and the electron configuration of the metal carbonyl are varied. The possibility of substituting the chloride in **1** by other anionic ligands allows probing the extent by which smaller electronic perturbations within the same class of complexes may modify the reaction energy of alkyl addition

(51) Carpenter, B. *Acc. Chem. Res.* **1992**, *25*, 520.

(52) This is a result from new calculations conducted to allow comparison between direct methyl−M bond formation in the $[RhPMe_3)_2CO)Cl]$ and $[RuCO)_5]$ systems.

Table 2. Substituent Effects on the Reaction Energy of Methyl Radical Addition, Ionization, and CO Bond Dissociation Energy of [*trans*-Rh(PMe$_3$)$_2$(CO)X]^a

	X	F	Cl	Br	I	CN
Rh-Me Product		ΔE for Methyl Addition to the Rh of [Rh(PMe$_3$)$_2$(CO)X]				
2a	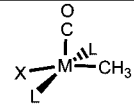	-8.0	-11.3	-12.3	-13.5	-10.5
2b	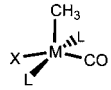	-10.3	-10.5	-11.5	-12.5	-12.7
2c	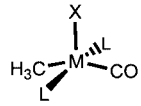	-3.8	-9.6	-12.2	-15.3	-7.8
Rh-Acyl Product		ΔE for Methyl Addition to the CO of [Rh(PMe$_3$)$_2$(CO)X]				
3a	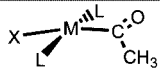	-11.7	-15.3	-16.8	-18.1	-11.3
3c	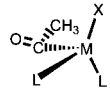	-9.9	-11.9	-13.3	-15.1	-8.3
Ionized Product		IE = Ionization Energy of [Rh(PMe$_3$)$_2$(CO)X]				
1$^+$($^2A_1$)	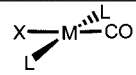	151.8	156.4	157.2	157.8	157.8
1$^+$($^2A''$)		153.2	156.6	156.8	156.7	160.5
CO Diss-Product		BDE = CO Bond Dissociation Energy of [Rh(PMe$_3$)$_2$(CO)X]				
T1	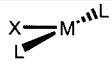	67.7	63.5	61.3	58.3	49.4
T2	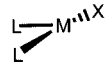	52.5	49.0	47.8	46.6	51.0

^{a} Units are in kcal/mol. All the molecules in the table were verified to be minima on the potential energy surface by normal mode analysis.

to a metal-coordinated carbonyl. Such study should also be useful to evaluate more critically the importance of the ionization and M−CO bond dissociation energies in radical addition to coordinated CO. In this section we consider methyl addition to the F, Br, I, and CN analogues of **1**. Because the energies of the accessible isomers and electronic states of the alkyl and acyl products in the reaction of **1** were not very different for the chloro complex, one cannot rule out the possibility that the relative energy of the different product species may switch when the substituents are varied. Accordingly, we ended up calculating all the molecules discussed in the reaction of the chloro complex for each of the new substituents (**3b** and **3d** are systematically higher in energy than **3a** and **3c**, respectively, so they are not included in the table). The results are summarized in Table 2. Although the collective data may look intimidating at first, the answer to the main question of interest to the present study can be readily extracted from the table. Most importantly, when X is a halogen, the lowest energy product is systematically the Rh−acyl product with the $^2A'$ state. (**3a**). Thus for this series the energy of formation **3a** from **1** and the methyl radical should provide a meaningful assessment of the effect of the halogen on the methyl affinity of the carbonyl in the given square-planar system. This issue is discussed later in the section. The rest of the data in Table 2 provide useful information on (i) the effects of substitution on the energy gap between the $^2A'$ and $^2A''$ states of the Rh−acyl product, **3a** vs **3c**, and (ii) the substituent effects on the energy difference between the alkyl and acyl products (**2** vs **3**).

Briefly, for all substituents, **3a** is uniformly lower in energy than **3c** (by 1.8–3.4 kcal/mol). For the halogen complexes, **3a** is also 1.4–4.5 kcal/mol lower in energy than the Rh−alkyl product. However, the relative energy of the three *trans*-Rh(PMe$_3$)$_2$ Rh−alkyl isomers considered in Table 1 (**2a**−**2c**) is found to depend on the identity of the halogen, although in all cases the energy difference between the isomers is small. For example, when X = F, the lowest energy Rh−alkyl isomer is **2b**, with CH_3 at the apical site of the square pyramid. For X = I on the other hand, the square-pyramidal geometry with the halogen at the apical site (**2c** in Table 2) becomes the preferred isomer. In contrast to the halogens, for the cyano substituent, the five-coordinate alkyl product is 1.4 kcal/mol more favored than the acyl product. Overall, therefore, the anionic substituent appears to have a minor effect on the relative energy order of the accessible electronic states and isomers in the given metal radical system.

For the purposes of the present study, the most important part of Table 2 is the one pertaining to the effect of the anionic ligand on methyl addition to the coordinated CO. Inspection of the data reveals that this addition reaction is more favored for the heavier halogen substituents. Thus, for X = F, $\Delta E = -11.7$ kcal/mol, making it is substantially less favored than the reaction of free CO ($\Delta E = -19.9$ kcal/mol, Table 1). Changing F into

Cl increases the reaction exothermicity by 3.6 kcal/mol. Subsequent substitution down the halogen group results in smaller incremental increases in the exothermicity, reaching −18.1 kcal/mol (ΔE) for X = I.

Table 2 examines if the methyl affinity trends correlate with either the ionization or the CO bond dissociation energy of **1**. For the halogen complexes, the IE is calculated to increase down the group, first in a large step and then in increments of near half a kcal/mol: IE = 151.8 (F) < 156.4 (Cl) < 157.2 (Br) < 157.8 (I) (in kcal/mol; Table 2). This is a counterintuitive trend that was noted in previous studies.[44,53] Clearly, the given IEs cannot rationalize the methyl affinity trends of the coordinated CO: the iodo complex is the hardest to ionize, but it is the complex that adds the alkyl radical most favorably. In accord with previous discussions, the given methyl affinities can be nicely related to the calculated Rh−CO BDEs: 67.7 (F) > 63.5 (Cl) > 61.3 (Br) > 58.3 (I) (leading to **T1**; Table 2), with the stronger Rh−CO bond (X = F, for example) exhibiting the smaller methyl affinity. However, when X = CN, the BDE is 49.0 kcal/mol, 8.7 kcal/mol less than the BDE for X = F, yet the exothermicity of methyl addition is comparable in the two complexes (ca. −11 kcal/mol, considering **3a** in Table 2). This is not necessarily disappointing since for the given pair of complexes the ionization energy is 6 kcal/mol greater for the cyano complex. Thus, when all the substituents are considered, the results demonstrate that both the IE and the Rh−CO BDE must be invoked to be able to account for the methyl affinity trends in the given system satisfactorily.

Conclusions

There is currently limited experimental or theoretical data on how coordination of an unsaturated organic substrate to a transition metal may influence the kinetics and thermodynamics of its reaction with free radicals. In the present work we have used density functional theory to study methyl addition to carbon monoxide coordinated to the [Rh(PMe$_3$)$_2$X] fragment. The present work complements an earlier study of alkyl radical addition to various classes of saturated 18-e metal carbonyl complexes.[19] The new calculations predict that CO binding to [Rh(PMe$_3$)$_2$X] reduces its methyl affinity by 2 to 8 kcal/mol, depending on the substituent. A potential energy surface for the reaction calculated for X = Cl shows the absence of a transition state for direct methyl attack onto the carbonyl of [Rh(PMe$_3$)$_2$(CO)X]. This contrasts with the 18-e metal carbonyl systems where the reactions encounter TSs even when there is a large driving force for the reaction. We attribute the different behavior of **1** to its square-planar geometry, which makes the Rh 4d$_{z^2}$ and 5p$_z$ AOs accessible to start a net bonding interaction with the methyl radical even at an early stage of the reaction, which seems to skew the region of C−C bond formation on the PES in the direction of Rh−C bond formation.

In an attempt to use the calculations to identify likely fundamental properties that can be used to account for the relative reaction and activation energies of their reaction with alkyl radicals, we noted that for all the 16-e and 18-e complexes considered so far the reaction is formally oxidative in the metal. We thus examined if the methyl affinity trends of the coordinated CO would follow the ionization energy of the metal carbonyls. When the collective data are considered, the results indicate strongly that a smaller ionization energy of the reacting metal carbonyl does not guarantee a more favored reaction. Further analysis of the results demonstrates that a satisfactory interpretation of the calculated methyl affinity trends can be achieved by considering both the ionization energy and the metal carbonyl bond strength at the same time. While low ionization energy intuitively suggests a more favorable oxidative reaction, an increase in the M−CO bond strength seems to disfavor the addition. Such interplay between metal-based (such as the IE) and metal–ligand-based (such as the BDE) properties identified in the reaction of coordinated CO should presumably have relevance to free radical addition to metal-coordinated ligands in general.

Acknowledgment. This work was funded by a grant from the University Research Board at the American University of Beirut and by NCSA Grant CHE030004. The work used computer resources donated by US-AID to the Center for Advanced Mathematical Sciences at AUB. Mahmoud Madi is thanked for help with using Mtlab. Prof. Alan Goldman is acknowledged for useful discussion. We also acknowledge useful comments from the referees.

Supporting Information Available: Tables of Cartesian coordinates and total B3LYP energies of the reactants, low-energy alkyl and acyl products, and the transition state connecting them. This material is available free of charge via the Internet at http://pubs.acs.org.

OM701079M

(53) Doherty, N. M.; Hoffman, N. W. *Chem. Rev.* **1991**, *91*, 553.